



OPEN Mechanism of miR-200b-3p-induced FOSL2 inhibition of endometrial cancer cell proliferation and metastasis

Lijie He¹, Zhongmin Jiang², Jing Wang¹ & Zhe Han¹✉

The purpose of this study was to investigate how miR-200b-3p inhibits the proliferation and metastasis of endometrial cancer cells by inducing the expression of FOSL2 in the AP1 transcription family. Endometrial cancer cell line HEC-1-A was divided into 16 groups: NC-mimic (transfected with negative control NC mimic), miR-200b-3p mimic (transfected with miR-200b-3p mimic), NC-suppress (transfected with negative control NC inhibit), miR-200b-3p inhibit group (transfected with miR-200b-3p inhibit), si-NC (transfected with negative control si-NC), si-FOSL2 (transfected with Si-FOSL2), oe-NC (transfected with negative control oe-NC), oe-FOSL2 group (oe-FOSL2), miR-200b-3p mimic + oe-NC group (co-transfected with miR-200b-3p mimic and oe-NC), miR-200b-3p mimic + oe-FOSL2 group (co-transfected with miR-200b-3p mimic and oe-FOSL2), miR-200b-3p inhibit + si-NC group (co-transfected with miR-200b-3p inhibit and si-NC), miR-200b-3p inhibit + si-FOSL2 group (co-transfected with miR-200b-3p inhibit and si-FOSL2), miR-200b-3p mimic + si-NC group (co-transfected with miR-200b-3p mimic and si-NC), miR-200b-3p mimic + si-FOSL2 group (co-transfected with miR-200b-3p mimic and si-FOSL2), miR-200b-3p inhibit + oe-NC group (co-transfected with miR-200b-3p inhibit and oe-NC), miR-200b-3p inhibit + oe-FOSL2 group (co-transfected with miR-200b-3p inhibit and oe-FOSL2). Real-time fluorescence quantitative PCR, Western blot, CCK-8 assay, scratch test and Transwell assay were used to detect the expression of miR-200b-3p mRNA, FOSL2 mRNA and protein, cell proliferation, migration and invasion. In endometrial cancer cell lines, the expression of miR-200b-3p was significantly down-regulated ($P < 0.05$), while the expression of FOSL2 was significantly up-regulated ($P < 0.05$). Compared with NC-mimic group, the expression of FOSL2, N-cadherin and Vimentin in miR-200b-3p mimic group was significantly decreased ($P < 0.05$), and the expression of E-cadherin was significantly increased ($P < 0.05$). The cell proliferation, migration rate and the number of transmembrane cells were significantly decreased ($P < 0.05$). Compared with the miR-200b-3p mimic + oe-NC group, the expression of FOSL2, N-cadherin and Vimentin in miR-200b-3p mimic + oe-FOSL2 was significantly increased ($P < 0.05$), the expression level of E-cadherin was significantly decreased ($P < 0.05$), and the cell proliferation, migration rate and the number of transmembrane cells were significantly increased ($P < 0.05$). Compared with NC-inhibit group, the expression of FOSL2, N-cadherin and Vimentin in miR-200b-3p inhibit group was significantly increased ($P < 0.05$), and the expression of E-cadherin was significantly decreased ($P < 0.05$). The cell proliferation, migration rate and the number of transmembrane cells were significantly increased ($P < 0.05$). Compared with the miR-200b-3p inhibit + si-NC group, the expression of FOSL2, N-cadherin and Vimentin in miR-200b-3p inhibit + si-FOSL2 was significantly decreased ($P < 0.05$), and the expression of E-cadherin was significantly increased ($P < 0.05$); the cell proliferation, migration rate and the number of transmembrane cells were significantly decreased ($P < 0.05$). The expression of miR-200b-3p in endometrial cancer cells is down-regulated, which can inhibit the proliferation, migration and invasion of endometrial cancer cells by regulating the EMT process, and its mechanism is related to its targeted negative regulation of FOSL2 expression.

Keywords miR-200b-3p, FOSL2, Endometrial cancer, Cell proliferation, Cell metastasis, EMT

¹Department of Clinical Laboratory, Tianjin Fifth Central Hospital, 41 Zhejiang Road, Tianjin 300450, People's Republic of China. ²Department of Pathology, Tianjin Fifth Central Hospital, Tianjin 300450, People's Republic of China. ✉email: hzxka123@163.com

Endometrial cancer (EC) is a malignant tumor that occurs in the endometrial lining of the female reproductive system, with adenocarcinoma being the most common type. The incidence of EC has been steadily increasing worldwide¹. Early treatment of EC is associated with relatively good prognosis²; however, patients with advanced or recurrent EC have a poor clinical outcome, with significantly reduced survival rates. The 5-year survival rates for patients with pelvic and extra-pelvic metastatic EC are 69% and 17%³, respectively. As the only gynecological malignancy with increasing mortality rates⁴, there is an urgent need to further explore the mechanisms underlying its occurrence and development. MicroRNAs (miRNAs) are small non-coding RNAs (ncRNAs) typically consisting of 19–24 nucleotides, which can directly influence or regulate intracellular signaling pathways and indirectly affect the expression of tumor-related proteins^{5–7}, thereby exerting either tumor-suppressive or tumor-promoting effects. Numerous miRNAs have been confirmed to be closely related to the occurrence and development of EC^{8,9}. Among them, miR-200b has been shown to affect cancer progression by regulating the epithelial-mesenchymal transition (EMT) process in EC cells¹⁰. miR-200b-3p, a member of the miR-200b family, has also been demonstrated to inhibit the proliferation, invasion, and migration capabilities of various tumors by suppressing the expression of downstream mRNAs^{11–13}.

FOS-like antigen 2 (FOSL2) is a member of the activator protein-1 (AP-1) transcription factor family, widely expressed in tissues, and plays a crucial role in regulating growth, development, and immune responses in both physiological and pathological processes¹⁴. Multiple studies have shown that FOSL2 can serve as a downstream target protein of miRNAs, regulating EMT, metastasis, and other processes that mediate the progression of malignant tumors^{15–17}. Although numerous studies have confirmed the important roles of miR-200b-3p and FOSL2 in the progression of various cancers, their roles in the occurrence and development of EC remain unclear. Therefore, this study aims to investigate how miR-200b-3p regulates FOSL2 and its effects on the proliferation and metastasis of EC cells, as well as to reveal its potential molecular mechanisms.

Material and methods

Cells and primary reagents

Human endometrial cancer (HEC-1-A, RL95-2, Ishikawa) and human normal endometrial mesenchymal hEM15A are purchased from the Shanghai Cell Bank, Chinese Academy of Sciences. 0.25% trypsin, trypsin, DMEM medium, RPMI 1640 medium, and RIPA lysate are purchased from Promega, USA. TRIzol (Invitrogen, USA). miR-200b-3p inhibitor, FOSL2 inhibitor, and β -actin are purchased from Thermo Fisher Scientific, USA. N-cadherin inhibitor, Vimentin inhibitor and human E-cadherin inhibitor are purchased from CST, USA. miR-200b-3p mimic, miR-200b-3p inhibitor, si-FOSL2, oe-FOSL2 and the corresponding negative control are purchased from Ribobio, China. wild-type FOSL2 3' UTR (FOSL2-WT), mutant FOSL2 3' UTR (FOSL2-WT) report vectors are purchased from Vigenebio, Shandong, China. The dual-luciferase reporter gene kit is purchased from Solarbio, USA. The CCK-8 reagent and the cell cycle kit are purchased from Beyotime Biotech Inc, Shanghai, China. Transwell chamber is purchased from Thermo, USA.

Cell culture and cell transfection

Endometrial cancer cell lines HEC-1-A, RL95-2, Ishikawa and human normal endometrial mesenchymal stromal cell line hEM15A were cultured in DMEM medium containing 10% fetal bovine serum (FBS) at 37°C with 5% CO₂ incubator. The HEC-1-A cell line was divided into 16 groups, and 3 replicate wells were set up in each group: NC-mimic (transfected with negative control NC mimic), miR-200b-3p mimic (transfected with miR-200b-3p mimic), NC-inhibit (transfected with negative control NC inhibit), miR-200b-3p inhibit group (transfected with miR-200b-3p inhibit), si-NC (transfected with negative control Si-NC), Si-FOSL2 (transfected with Si-FOSL2), oe-NC (transfected with negative control oe-NC), oe-FOSL2 group (oe-FOSL2), miR-200b-3p mimic + oe-FOSL2 group (co-transfected with miR-200b-3p mimic and oe-FOSL2), miR-200b-3p inhibit + si-NC group (co-transfected with miR-200b-3p inhibit and si-NC), miR-200b-3p inhibit + si-FOSL2 group (co-transfected with miR-200b-3p inhibit and si-FOSL2), miR-200b-3p mimic + si-NC group (co-transfected with miR-200b-3p mimic and si-NC), miR-200b-3p mimic + si-FOSL2 group (co-transfected with miR-200b-3p mimic and si-FOSL2), miR-200b-3p inhibit + oe-NC group (co-transfected with miR-200b-3p inhibit and oe-NC), miR-200b-3p inhibit + oe-FOSL2 group (co-transfected with miR-200b-3p inhibit and oe-FOSL2) (Table 1). The miR-200b-3p mimic, miR-200b-3p inhibitor, si-FOSL2, oe-FOSL2, and the corresponding negative control were individually or co-transfected into HEC-1-A cells using the Lipofectamine 2000 kit according to the instructions. 48h later, the transfection efficiency was verified by real-time fluorescence quantitative PCR and Western blot to verify the transfection efficiency.

Real-time fluorescence quantitative PCR

Total RNA was extracted using TRIzol reagent, and the RNA concentration and OD₂₆₀/OD₂₈₀ ratio were detected using a NanoDrop ultraviolet spectrophotometer. 10 μ g of RNA was taken and reverse transcribed into cDNA, and RT-qPCR was performed using SYBR Green Mix (Thermo Fisher Scientific, USA). β -actin was used as an internal reference, and the relative gene expression was calculated using the $-\Delta\Delta$ CT method. Three parallels were set in each group.

Western blot

Total protein was extracted using RIPA protein lysate containing 100 \times Cocktail and 100 \times PMSF, and protein concentration was determined by BCA protein assay kit. Proteins were electrophoretic transferred to PVDF membranes by 10% SDS-PAGE gel. After the transfer was completed, the membrane was closed with 5% skimmed milk for 1h at room temperature and incubated with the corresponding primary antibody at 4°C overnight. The membrane was washed with TBST buffer and incubated with the corresponding secondary antibody at room

Group	Treatment method
NC-mimic	Transfected with negative control NC mimic
miR-200b-3p mimic	Transfected with miR-200b-3p mimic
NC-inhibit	Transfected with negative control NC inhibit
miR-200b-3p inhibit	Transfected with miR-200b-3p inhibit
si-NC	Transfected with negative control si-NC
si-FOSL2	Transfected with si-FOSL2
oe-NC	Transfected with negative control oe-NC
oe-FOSL2	Transfected with oe-FOSL2
miR-200b-3p mimic + oe-NC	Co-transfected with miR-200b-3p mimic and oe-NC
miR-200b-3p mimic + oe-FOSL2	Co-transfected with miR-200b-3p mimic and oe-FOSL2
miR-200b-3p inhibit + si-NC	Co-transfected with miR-200b-3p inhibit and si-NC
miR-200b-3p inhibit + si-FOSL2	Co-transfected with miR-200b-3p inhibit and si-FOSL2
miR-200b-3p mimic + si-NC	Co-transfected with miR-200b-3p mimic and si-NC
miR-200b-3p mimic + si-FOSL2	Co-transfected with miR-200b-3p mimic and si-FOSL2
miR-200b-3p inhibit + oe-NC	Co-transfected with miR-200b-3p inhibit and oe-NC
miR-200b-3p inhibit + oe-FOSL2	Co-transfected with miR-200b-3p inhibit and oe-FOSL2

Table 1. Summary of treatment groups.

temperature for 1h. ECL reagent and chemiluminescence detection kit were used for blot analysis, β -actin was used as the internal control, and Image J v1.8 was used for blot analysis.

Bioinformatics analysis

Starbase (<http://starbase.sysu.edu.cn/index.php>) was used to predict the potential binding site between miR-200b-3p and FOSL2 3'-UTR.

Dual luciferase test

HEC-1A cells were co-transfected with Lipofectamine 2000 (miR-200b-3p mimic /NC mimic), wild-type FOSL2 3'UTR (FOSL2-WT), mutant FOSL2 3'-UTR (FOSL2-MUT), ETV1 3'UTR (ETV1-WT), mutant ETV1 3'-UTR (ETV1-MUT), EGFR 3'UTREGFR (EGFR-WT), mutant EGFR 3'-UTR (EGFR-MUT). After 48h of transfection, luciferase activity was measured using Dual-Lucy Assay Kit.

Cell proliferation assay

The CCK-8 method was used to detect the proliferation of EC cells. Logarithmically growing HEC-1-A cells were prepared into a cell suspension of 5×10^4 cells/mL. 100 μ L of the cell suspension was inoculated into a 96 well plate at 37 °C, Cultivate for 2–3 h under 50 mL/L CO₂ conditions; Subsequently, add 10 μ L of CCK-8 reagent to each well and continue culturing for 2 h. Measure the absorbance (A) value at 450 nm, record the data, and plot the cell proliferation curve.

Cell scratch assay

Cell migration was detected using the cell scratch assay. EC cells were inoculated in 6-well plates at a density of 1×10^5 cells/well, and when the cell fusion reached more than 80%, a 200 μ L tip was used to scratch vertically at the bottom of the well plates to form cell scratches. After completion of the scratch, the cells were rinsed with PBS to remove the suspended cells. Add 20 μ L of 1 mg/mL Mitomycin C to 2 mL of culture medium in each well to achieve a final concentration of 10 μ g/mL. Incubate cells in a medium containing Mitomycin C for 2 h to inhibit cell proliferation. After incubation, aspirate the medium containing Mitomycin C, gently wash the cells twice with PBS, and then add fresh medium. Photographs were taken at 0 h and 24 h after scratching with a $10 \times$ field of view. The area of the scratch at each time point was analyzed using ImageJ software, and the mobility rate was calculated.

Transwell detection

Cell invasion was detected using the Transwell assay. HEC-1A cells were inoculated at a density of 1×10^5 cells/well in the upper chamber of a small chamber containing 200 μ L of serum-free medium, while 500 μ L of medium containing 10% fetal bovine serum was added to the lower chamber. After 24 h of incubation at 37 °C with 5% CO₂, cells remaining on the upper surface of the filter were removed, and cells migrating to the lower chamber were fixed using methanol and stained with crystal violet. Subsequently, five fields of view were randomly selected under a light microscope ($10 \times$ objective), and the average cell number was calculated.

Immunofluorescence

Cells were fixed with 4% paraformaldehyde for 15 min and permeabilized with 0.3% Triton X-100 for 15 min. Then, they were blocked with 5% goat serum at room temperature for 1 h. Next, the cells were incubated with the primary antibody overnight at 4 °C, followed by incubation with the corresponding secondary antibody for

1 h. Subsequently, DAPI staining was performed, and the expression and subcellular localization of the target protein were observed under a confocal fluorescence microscope.

Animal study and ethics

In the current study, 20 male BALB/c nude mice (4 weeks of age; average body mass 220–250 g) were obtained from the Tianjin Fifth Central Hospital, Central Laboratory. The nude mice were maintained under standard situations (a 12 h light/12 h dark cycle and at a temperature of 23–25 °C) at the animal lab and allowed free food and water intake ad libitum until the procedures started. All animal care and experimental protocols were approved by the ethics committee of Tianjin Fifth Central Hospital. (Ethics code: ZN-EC-001-3.3-FJ06) with an approval date of 2023/01/01. We confirmed that all methods were carried out under relevant guidelines and regulations. Moreover, we confirmed that all methods are reported following ARRIVE guidelines (<https://arriv eguidelines.org>).

Nude mouse xenograft tumor model

The experimental procedures and animal care were conducted in accordance with animal experimentation guidelines and approved by the ethics committee. si-Fosl2 was transfected into HEC-1-A cells, and approximately 5×10^6 cells were subcutaneously injected into 4-week-old male BALB/c nude mice to establish the mouse xenotransplantation model. After 4 weeks of tumor development, under halothane anesthesia, tumor harvesting from experimental mice. Tumor tissues were then harvested for subsequent histological and molecular biological analyses. The tumor volume was calculated using the following formula: V (volume) = L (length) \times W (width)² \times 0.52. Tumor volume was measured every three days. At the end of the experiment, the mice were euthanized, and all tumors were dissected and weighed. A luminescence imaging system was used to quantify the tumor cells in the nude mice.

HE staining

After deparaffinization and rehydration of tumor tissue paraffin sections, the sections were stained with hematoxylin for 3–5 min and then washed with water. They were differentiated in 1% HCl-75% ethanol for 5–10 s and washed with water. Next, they were treated with alkaline water to promote bluing for 20 s and washed with water again. The sections were then stained with eosin for 30–60 s and washed with water. They were subsequently rinsed with 80% ethanol for 3–5 s, 95% ethanol for 3–5 s, and absolute ethanol for 3–5 s. Finally, after mounting, the pathological changes in the tumor tissue were observed under an inverted microscope.

Statistical analysis

GraphPad Prism statistical software is applied to analyze the data and plot. Data in this study are expressed as mean \pm SD. t-test, one-way ANOVA and SNK-q test were used for comparison of measurement data. $P < 0.05$ is considered as significant statistically difference.

Results

miR-200b-3p mimic and FOSL2 expression in EC cells

Compared to normal human endometrial cells, the expression level of miR-200b-3p is significantly downregulated in EC cell lines, with the lowest expression observed in HEC-1-A (Table 2, Fig. 1A). This cell line was chosen for subsequent overexpression experiments. The mRNA and protein expression levels of FOSL2 are significantly increased in EC cell lines ($P < 0.05$, Fig. 1B, C). Using Starbase, potential binding sites between miR-200b-3p and FOSL2 3'-UTR were predicted (Fig. 1D). Compared to the NC-inhibitor group, the expression of miR-200b-3p is significantly reduced in the miR-200b-3p inhibitor group, while the expression level of miR-200b-3p is significantly increased in the miR-200b-3p mimic group compared to the NC-mimic group (Table 3, Fig. 1E). The results of the dual luciferase assay show that the dual luciferase activity of the FOSL2-WT vector in the miR-200b-3p mimic group is significantly reduced compared to the NC-mimic group ($P < 0.01$, Table 4, Fig. 1G). Compared with the NC group, after overexpression of miR-200b-3p, the relative expression level of FOSL2 mRNA was significantly downregulated. After knocking down miR-200b-3p, the relative expression level of FOSL2 mRNA was significantly upregulated ($P < 0.01$, Table 5, Fig. 1F).

The regulatory mechanism of miR-200b-3p on FOSL2

Compared to the si-NC group, the expression of FOSL2 mRNA and protein is significantly reduced in the si-FOSL2 group; compared to the oe-NC group, the expression of FOSL2 mRNA and protein is significantly increased in

Groups	miR-200b-3p	FOSL2 mRNA	FOSL2
hEM15A	1.01 \pm 0.02	0.49 \pm 0.02	0.58 \pm 0.03
HEC-1-A	0.31 \pm 0.04 ^b	1.24 \pm 0.04 ^b	1.26 \pm 0.11 ^b
RL95-2	0.49 \pm 0.04 ^b	1.18 \pm 0.12 ^b	1.13 \pm 0.08 ^b
Ishikawa	0.61 \pm 0.02 ^b	0.67 \pm 0.06 ^b	0.74 \pm 0.03 ^b
F	792.900	248.940	181.759
P	$P < 0.001$	$P < 0.001$	$P < 0.001$

Table 2. miR-200b-3p mRNA and protein expression in EC cell lines (n = 3, $\bar{x} \pm s$). ^b $P < 0.01$ versus hEM15A cell.

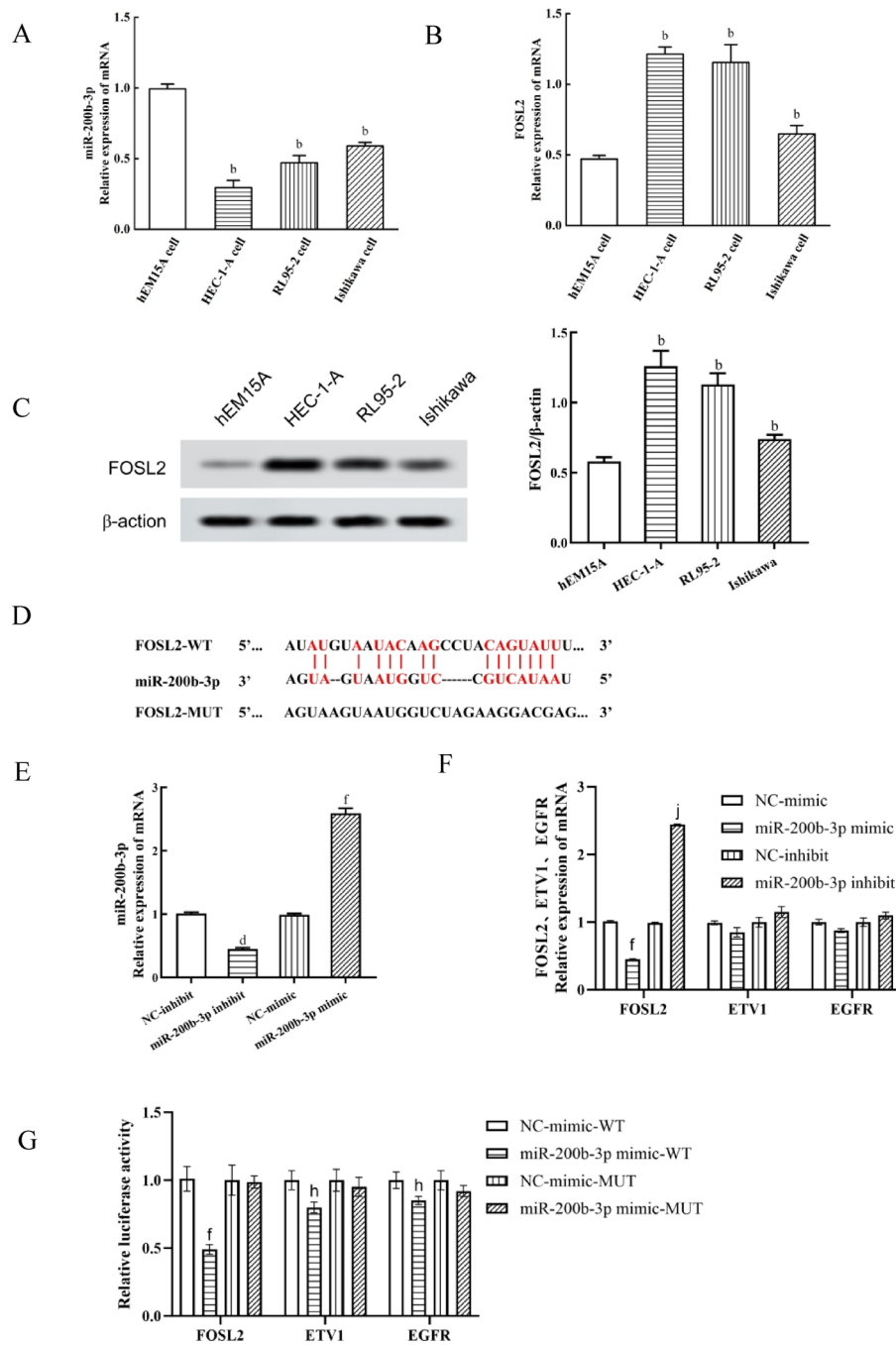


Fig. 1. The mRNA and protein expression levels of FOSL2 in EC cells and the targeted binding sites of miR-200b-3p with the FOSL2 3'-UTR. **(A)** Expression of miR-200b-3p in EC cell lines; **(B)** Semi-quantitative analysis of FOSL2 mRNA expression in EC cell lines; **(C)** Protein expression levels of FOSL2 in EC cell lines and semi-quantitative analysis; ^b*P* < 0.01 versus hEM15A cell. **(D)** Target binding sites of miR-200b-3p in the 3'-UTR of FOSL2; **(E)** Expression of miR-200b-3p in various groups of cells; ^d*P* < 0.01 versus NC-inhibitor group. **(F)** Expression of FOSL2, ETV1, EGFR in various groups of cells; ^f*P* < 0.01 versus NC-mimic group; ^j*P* < 0.01 versus NC-inhibitor. **(G)** Results of dual luciferase assay. ^f*P* < 0.01 versus NC-mimic group; ^h*P* < 0.05 versus NC-mimic group.

the oe-FOSL2 group (*P* < 0.01, Figs. 2A, B, Table 6). Compared to the NC-mimic group, the expression of FOSL2 mRNA and protein is significantly reduced in the miR-200b-3p mimic group; compared to the miR-200b-3p mimic combined with oe-NC group, the expression of FOSL2 mRNA and protein is significantly increased in the miR-200b-3p mimic combined with oe-FOSL2 group. Compared to the NC-inhibitor group, the expression of FOSL2 mRNA and protein is significantly increased in the miR-200b-3p inhibitor group; compared to the miR-200b-3p inhibitor combined with si-NC group, the expression of FOSL2 mRNA and protein is significantly

Groups	miR-200b-3p
NC-inhibit	1.01 ± 0.02
miR-200b-3p inhibit	0.45 ± 0.02 ^d
t	33.607
P	< 0.001
NC-mimic	0.99 ± 0.02
miR-200b-3p mimic	2.59 ± 0.08 ^f
t	34.293
P	< 0.001

Table 3. miR-200b-3p mRNA expression in each group of cells (n = 3, x ± s). ^dP < 0.01 versus NC-inhibit group; ^fP < 0.01 versus NC-mimic group.

Groups	FOSL2-WT	FOSL2-MUT	ETV1-WT	ETV1-MUT	EGFR-WT	EGFR-MUT
NC-mimic	1.01 ± 0.09	1.00 ± 0.11	1.00 ± 0.07	1.00 ± 0.08	1.00 ± 0.06	1.00 ± 0.07
miR-200b-3p mimic	0.49 ± 0.05 ^f	0.99 ± 0.08	0.80 ± 0.06 ^h	0.95 ± 0.09	0.85 ± 0.05 ^h	0.92 ± 0.06
t	8.748	0.127	3.76	0.722	3.331	1.501
P	0.001	0.905	0.020	> 0.05	0.030	> 0.05

Table 4. Dual luciferase assay (n = 3, x ± s). ^fP < 0.01 versus NC-mimic group; ^hP < 0.05 versus NC-mimic group.

Groups	FOSL2	ETV1	EGFR
NC-mimic	1.01 ± 0.01	1.00 ± 0.07	1.00 ± 0.06
miR-200b-3p mimic	0.45 ± 0.02 ^f	0.85 ± 0.09	0.88 ± 0.07
t	43.377	2.283	2.261
P	< 0.001	0.08	0.09
NC-inhibit	0.99 ± 0.02	1.00 ± 0.08	1.00 ± 0.09
miR-200b-3p inhibit	2.44 ± 0.03 ⁱ	1.15 ± 0.12	1.10 ± 0.10
t	69.656	1.801	1.295
P	< 0.001	0.071	0.060

Table 5. Expression of FOSL2, ETV1, EGFR mRNA in each group of cells (n = 3, x ± s). ^fP < 0.01 versus NC-mimic group; ⁱP < 0.01 versus NC-inhibitor.

reduced in the miR-200b-3p inhibitor combined with si-FOSL2 group ($P < 0.01$, Figs. 2C, D, Table 7). Compared to the miR-200b-3p mimic combined with si-NC group, the expression of FOSL2 mRNA and protein is significantly increased in the miR-200b-3p mimic combined with si-FOSL2 group ($P < 0.01$, Fig. 2E).

Effect of miR-200b-3p on endometrial cancer cell proliferation, migration and invasion

Compared with the NC-mimic group, showed a significant decreased the cell proliferation activity, cell migration rate, and the number of membrane-penetrating cells in the miR-200b-3p mimic group were significantly decreased ($P < 0.05$), the mRNA and protein expression levels of the epithelial markers, N-cadherin and Vimentin were significantly decreased ($P < 0.05$), and the mRNA and protein expression levels of mesenchymal marker were significantly increased ($P < 0.05$). Compared with the miR-200b-3p mimic + oe-NC group, cell proliferation activity, cell migration rate, and number of membrane-penetrating cells in the miR-200b-3p mimic + oe-FOSL2 group were significantly increased ($P < 0.05$), the mRNA and protein expression levels of N-cadherin and Vimentin were significantly increased ($P < 0.05$), and the mRNA and protein expression levels of E-cadherin's mRNA and protein expression levels were significantly decreased ($P < 0.05$). Compared with the NC-inhibit group, the cell proliferation activity, cell migration rate, and number of membrane-penetrating cells in the miR-200b-3p inhibit group were significantly increased ($P < 0.05$), the mRNA and protein expression levels of N-cadherin and Vimentin were significantly increased ($P < 0.05$), and the mRNA and protein expression levels of E-cadherin were significantly decreased ($P < 0.05$). Compared with the miR-200b-3p inhibit + si-NC group, the cell proliferative activity, cell migration rate, and the number of membrane-penetrating cells in the miR-200b-3p inhibit + si-FOSL2 group were significantly decreased ($P < 0.05$), mRNA and protein expression levels of N-cadherin and Vimentin were significant decreased ($P < 0.05$), and the mRNA and protein expression levels of E-cadherin were significant increased ($P < 0.05$), (Fig. 3, Tables 8 and 9).

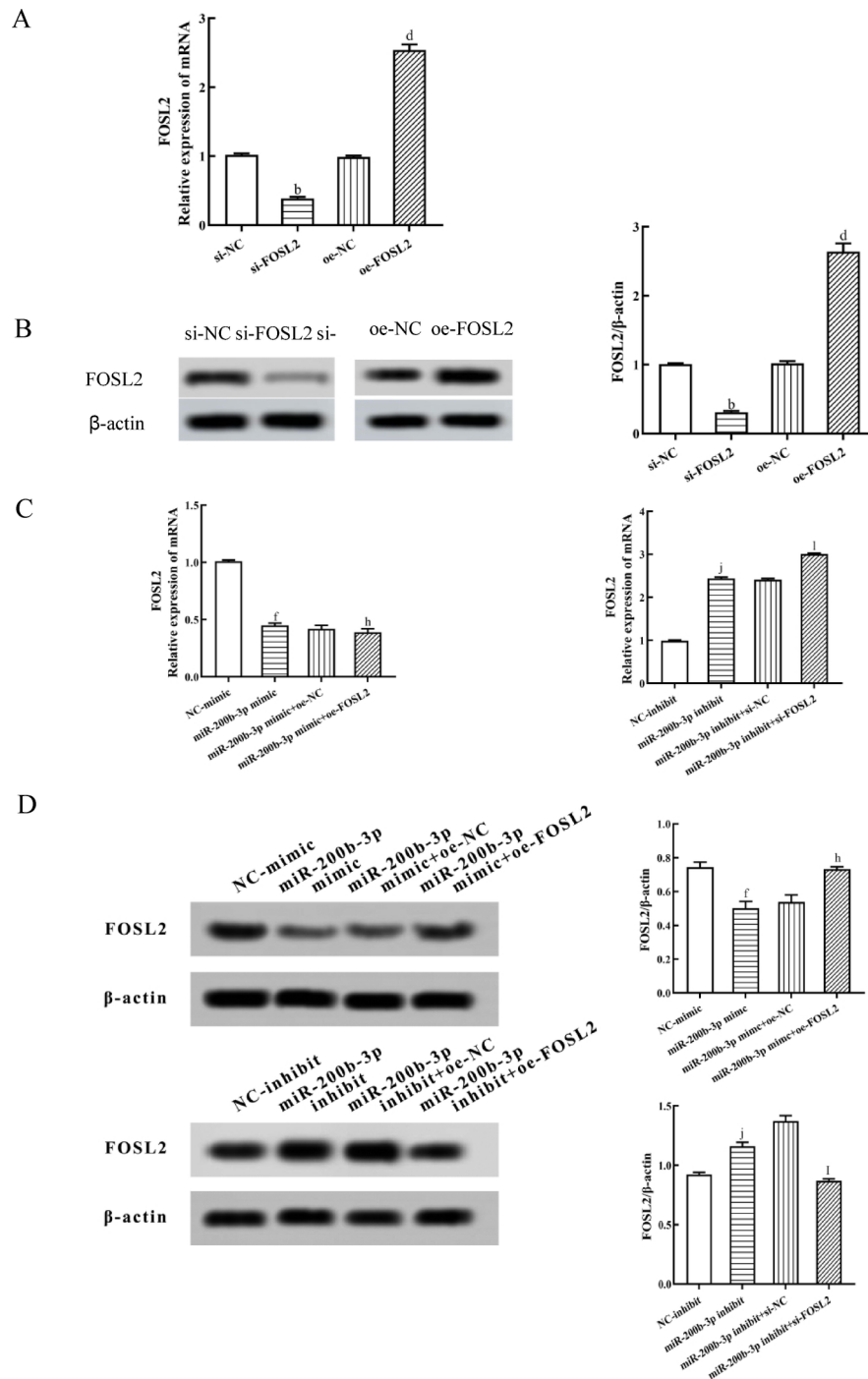


Fig. 2. The regulatory mechanism of miR-200b-3p on FOSL2. **(A)** The mRNA expression levels of FOSL2 in overexpression and knockdown constructs; **(B)** The protein expression levels of FOSL2 in overexpression and knockdown constructs and semi-quantitative analysis; **(C)** The mRNA expression levels of FOSL2 in recovery cells; **(D)** The protein expression levels of FOSL2 in recovery cells and semi-quantitative analysis. **(E)** Immunofluorescence staining. ^b $P < 0.01$ versus si-NC group; ^d $P < 0.01$ versus oe-NC group; ^f $P < 0.01$ versus NC-mimic group; ^h $P < 0.01$ versus miR-200b-3p mimic combined with oe-NC group; ^j $P < 0.01$ versus NC-inhibitor group; ^l $P < 0.01$ versus miR-200b-3p inhibitor combined with si-NC group; ^{*} $P < 0.01$, ^{**} $P < 0.001$.

Downregulation of FOSL2 exerts a tumor-suppressive

Based on the tumor growth curve, it can be observed that compared to the NC-inhibit group, the miR-200b-3p-inhibit group shows a significant slowdown in the tumor volume increase, with a marked reduction in tumor volume ($P < 0.01$, Fig. 4A, B, C). This directly reflects that the knockout of miR-200b-3p inhibits the proliferation of tumor cells. The decrease in tumor volume may be related to cell cycle arrest, enhanced apoptosis, or changes in the tumor micro environment. HE staining of tumor tissues showed that the si-FOSL2 group exhibited a more

E

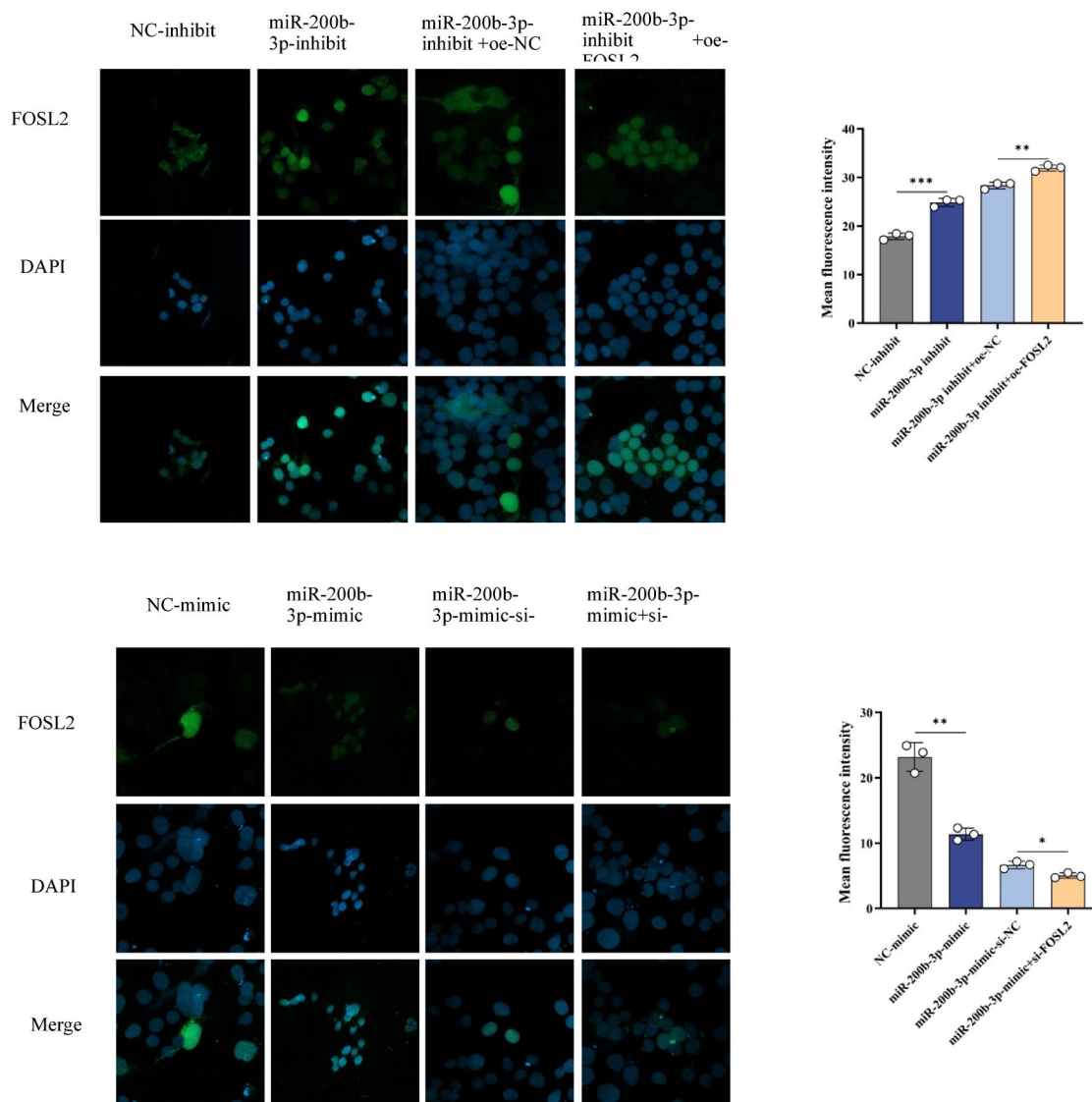


Figure 2. (continued)

Groups	FOSL2 mRNA	FOSL2
si-NC	1.02 ± 0.02	1.01 ± 0.01
si-FOSL2	0.39 ± 0.02 ^b	0.31 ± 0.02 ^b
t	38.579	54.222
P	< 0.001	< 0.001
oe-NC	0.99 ± 0.02	1.02 ± 0.03
oe-FOSL2	2.54 ± 0.08 ^d	2.64 ± 0.12 ^d
t	32.557	23.105
P	< 0.001	< 0.001

Table 6. Expression of FOSL2 mRNA and protein in each group of cells (n = 3, x ± s). ^bP < 0.01 versus si-NC; ^dP < 0.05 versus oe-NC.

Groups	FOSL2 mRNA	FOSL2
NC-mimic	1.01 ± 0.01	0.99 ± 0.01
miR-200b-3p mimic	0.45 ± 0.02 ^f	0.39 ± 0.02 ^f
t	43.377	46.476
P	<0.001	<0.001
miR-200b-3p mimic + oe-NC	0.42 ± 0.03	0.40 ± 0.02
miR-200b-3p mimic + oe-FOSL2	0.39 ± 0.03 ^h	0.32 ± 0.02 ^h
t	19.188	20.176
P	<0.001	<0.001
NC-inhibit	0.99 ± 0.02	1.00 ± 0.02
miR-200b-3p inhibit	2.44 ± 0.03 ^j	2.40 ± 0.02 ^j
t	69.656	85.732
P	<0.001	<0.001
miR-200b-3p inhibit + si-NC	2.41 ± 0.03	2.38 ± 0.03
miR-200b-3p inhibit + si-FOSL2	3.01 ± 0.02 ^l	2.88 ± 0.05 ^l
t	33.627	21.090
P	<0.001	<0.001

Table 7. Expression of FOSL2 mRNA and protein in each group of cells (n = 3, x ± s). ^fP < 0.01 versus NC-mimic; ^hP < 0.01 us miR-200b-3pmimic + si-NC; ^jP < 0.01 versus NC-inhibitor; ^lP < 0.01 versus miR-200b-3p inhibitor + si-NC.

severe degree of necrosis compared to the si-NC group, The black arrow indicates necrotic tumor cells, while the blue arrow indicates normal tumor cells (P < 0.01, as shown in Fig. 4D). This necrotic phenomenon may lead to the suppression of tumor cell growth, thereby affecting tumor growth and metastasis.

Discussion

In this study, we explored the expression pattern and functional role of miR-200b-3p in EC cells, and found that miR-200b-3p was significantly downregulated in EC cells. This finding is consistent with previous studies in malignant tumors such as gastric cancer¹⁸, bladder cancer¹⁹, and small cell lung cancer²⁰. These cross-cancer studies collectively reveal the universality of miR-200b-3p as a potential tumor suppressor, suggesting that its downregulation may be one of the common mechanisms in the occurrence and development of various cancers. In this study, we demonstrated the inhibitory effect of miR-200b-3p on the proliferation of EC cells, which aligns with previous research on the regulatory role of miR-200b-3p in tumor proliferation. For instance, studies have shown that miR-200b-3p can inhibit tumor cell proliferation, apoptosis, invasion, and migration by silencing the mRNA expression of genes such as microfibril-associated glycoprotein 2 (MAGP2), mothers against DPP homolog 2 (SMAD2), and high mobility group protein B3 (HMGB3)¹¹. Wang et al.²¹ also demonstrated that miR-200b-3p accelerates tumor progression by negatively regulating the expression of reversion-inducing cysteine-rich kazal motif-containing protein (RECK). Additionally, our results support the hypothesis that miR-200b-3p can inhibit the invasion and migration of EC cells by regulating specific target genes. Recent studies have shown that miR-200b (including its mature form miR-200b-3p) can inhibit the epithelial-mesenchymal transition process in EC cells by promoting the expression of naked cuticle homolog 2 (NKD2), thereby regulating the invasion and migration capabilities of cancer cells. Gyvyte et al.²² also found that miR-200b-3p can inhibit the invasion and migration of cancer cells by regulating the expression of ETS variant transcription factor 1 (ETV1) protein in gastrointestinal stromal tumors, which is consistent with our experimental results. This study indicates that, FOSL2 is a direct target of miR-200b-3p with high regulatory specificity. Although ETV1 and EGFR may also be regulated by miR-200b-3p, their effects are not as significant as FOSL2. This suggests that miR-200b-3p may act as a tumor suppressor gene to inhibit the proliferation and metastasis of EC cells.

In this study, we confirmed that FOSL2 is a direct target gene of miR-200b-3p through bioinformatics prediction using the Starbase database, combined with dual-luciferase reporter gene assays. This is consistent with previous studies indicating that members of the miR-200 family can target various genes associated with cancer progression, thereby exerting their tumor-suppressive functions¹¹. In particular, FOSL2, as a member of the Fos family, is an important component of the activator protein-1 (AP-1) transcriptional complex and has been shown to exhibit oncogenic effects in various cancers, including EC and ovarian cancer²³. Our results further support the role of FOSL2 as an oncogene in EC and reveal the molecular mechanism by which miR-200b-3p suppresses the malignant phenotype of EC cells through negative regulation of FOSL2. Additionally, we found that the inhibitory effects of miR-200b-3p on the proliferation, invasion, and migration of EC cells could be abolished by the overexpression of FOSL2, while the knockdown of miR-200b-3p enhanced these malignant phenotypes, and this effect was reversed following FOSL2 silencing. This result not only confirms the functional connection between miR-200b-3p and FOSL2 but also further emphasizes the tumor-suppressive role of miR-200b-3p in EC cells. This is consistent with the findings of Ma et al.²⁴. In colorectal cancer, where they found that miR-619-5p inhibits tumor cell proliferation and migration by targeting FOSL2. Gao et al.²⁵ also discovered that FOSL2, when targeted by miRNA-597-3p, further inhibits the proliferation of skin squamous cell carcinoma.

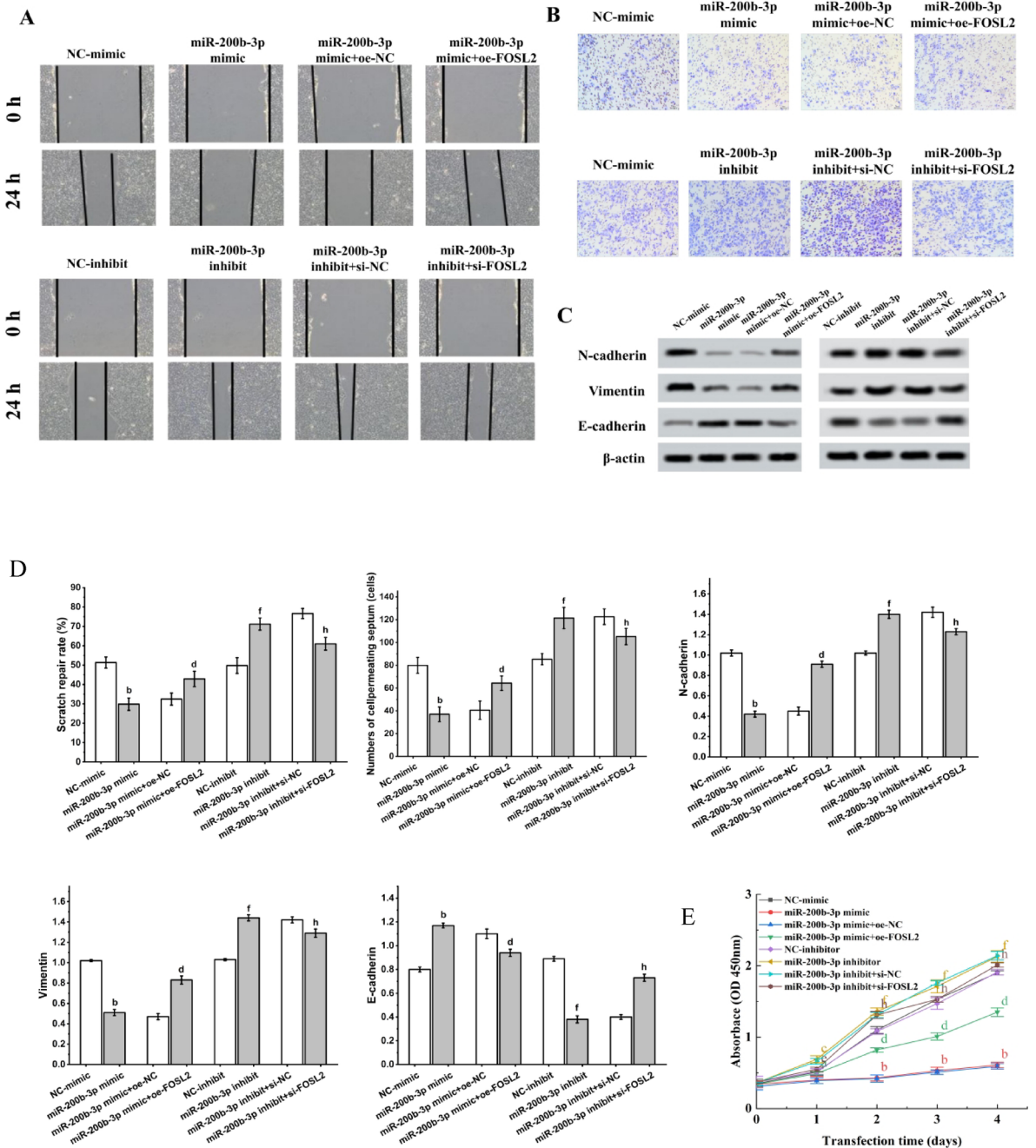


Fig. 3. Effect of miR-200b-3p on proliferation, migration and invasion of endometrial cancer cells. (A) cell scratch assay to detect cell migration; (B) Transwell assay to detect cell invasion; (C) Western blot to detect the expression of EMT marker proteins in tumor tissues; (D) Comparison of cell migration, invasion and EMT-related protein expression; (E) CCK-8 survival curve; ^b*P* < 0.01 versus NC-mimic; ^a*P* < 0.05, ^d*P* < 0.01 versus miR-200b-3p mimic + oe-NC; ^e*P* < 0.05 ^f*P* < 0.01, versus NC-inhibitor; ^e*P* < 0.05 ^h*P* < 0.01, versus NC-inhibitor.

Although these studies focus on different cancer types and miRNAs, they collectively reveal the important role of the miRNA-FOSL2 axis in cancer progression.

Epithelial-mesenchymal transition (EMT) refers to the process by which epithelial cells lose their original polarity and intercellular adhesion, gaining the ability to invade and migrate through the stroma. This process is characterized by a decrease in epithelial markers such as E-cadherin and β-catenin, and an increase in mesenchymal markers such as N-cadherin and Vimentin^{26,27}. EMT has been reported to be involved in the invasion and metastasis of various tumors, including EC²⁸. Studies have found that miR-200b-3p can inhibit EMT and thus tumor progression by targeting zinc finger E-box binding homeobox 1/2 (ZEB1/2)¹¹. In triple-negative breast cancer, miR-200b-3p can enhance the expression of epithelial cadherin (Cadherin-1, CDH1) and inhibit EMT by targeting the Rho GDP dissociation inhibitor (RHOGDI) signaling pathway²⁹. In this study, we

Groups	OD (450 nm)				
	0 d	1 d	2 d	3 d	4 d
NC-mimic	0.35 ± 0.06	0.51 ± 0.05	1.10 ± 0.05	1.53 ± 0.04	1.90 ± 0.03
miR-200b-3p mimic	0.34 ± 0.04	0.40 ± 0.05	0.43 ± 0.04 ^b	0.53 ± 0.05 ^b	0.61 ± 0.04 ^b
t	0.600	2.694	18.124	27.050	44.687
P	0.581	0.054	<0.001	<0.001	<0.001
miR-200b-3p mimic + oe-NC	0.31 ± 0.05	0.39 ± 0.04	0.42 ± 0.05	0.51 ± 0.03	0.59 ± 0.04
miR-200b-3p mimic + oe-FOSL2	0.34 ± 0.03	0.49 ± 0.02 ^a	0.82 ± 0.03 ^d	1.01 ± 0.05 ^d	1.35 ± 0.06 ^d
t	0.891	3.873	11.882	14.852	18.255
P	0.423	0.018	<0.001	<0.001	<0.001
NC-inhibit	0.37 ± 0.08	0.52 ± 0.04	1.08 ± 0.04	1.47 ± 0.08	1.91 ± 0.04
miR-200b-3p inhibit	0.36 ± 0.03	0.69 ± 0.05 ^c	1.36 ± 0.05 ^f	1.71 ± 0.09 ^f	2.13 ± 0.08 ^f
t	0.203	4.599	10.046	3.452	4.260
P	0.849	0.010	0.002	0.026	0.13
miR-200b-3p inhibit + si-NC	0.36 ± 0.03	0.66 ± 0.04	1.31 ± 0.04	1.76 ± 0.03	2.14 ± 0.06
miR-200b-3p inhibit + oe-FOSL2	0.37 ± 0.02	0.55 ± 0.03 ^e	1.13 ± 0.05 ^h	1.53 ± 0.04 ^h	2.01 ± 0.03 ^h
t	0.480	4.260	4.869	7.967	3.357
P	0.656	0.019	0.008	0.001	0.028

Table 8. Proliferative activity of each group of cells detected by CCK-8 assay (n = 3, x ± s). ^bP < 0.01 versus NC-mimic; ^aP < 0.05, ^dP < 0.01 versus miR-200b-3p mimic + oe-NC; ^cP < 0.05 ^fP < 0.01, versus NC-inhibitor; ^eP < 0.05 ^hP < 0.01, versus NC-inhibitor.

Groups	Scratch repair rate (%)	Numbers of cell permeating septum (cells)	N-cadherin	Vimentin	E-cadherin
NC-mimic	51.31 ± 2.87	79.89 ± 7.03	1.02 ± 0.03	1.02 ± 0.01	0.80 ± 0.02
miR-200b-3p mimic	29.84 ± 3.21 ^b	36.97 ± 6.49 ^b	0.42 ± 0.03 ^b	0.51 ± 0.03 ^b	1.17 ± 0.02 ^b
t	8.636	7.770	24.495	27.934	22.658
P	<0.001	0.001	<0.001	<0.001	<0.001
miR-200b-3p mimic + oe-NC	32.46 ± 3.11	40.59 ± 8.03	0.45 ± 0.04	0.47 ± 0.03	1.10 ± 0.04
miR-200b-3p mimic + oe-FOSL2	42.89 ± 3.98 ^d	64.28 ± 6.32 ^d	0.91 ± 0.03 ^d	0.83 ± 0.04 ^d	0.94 ± 0.03 ^d
t	3.577	4.015	15.935	12.471	5.543
P	0.023	0.016	<0.001	<0.001	<0.001
NC-inhibit	49.79 ± 4.11	85.31 ± 4.86	1.02 ± 0.02	1.03 ± 0.01	0.89 ± 0.02
miR-200b-3p inhibit	71.16 ± 3.15 ^f	121.40 ± 9.35 ^f	1.40 ± 0.04 ^f	1.44 ± 0.03 ^f	0.38 ± 0.03 ^f
t	3.148	5.932	14.717	22.457	24.500
P	0.002	0.004	<0.001	<0.001	<0.001
miR-200b-3p inhibit + is-NC	76.59 ± 2.62	122.59 ± 6.83	1.42 ± 0.05	1.42 ± 0.03	0.40 ± 0.02
miR-200b-3p inhibit + is-FOSL2	60.97 ± 3.28 ^h	105.18 ± 7.12 ^h	1.23 ± 0.03 ^h	1.22 ± 0.04 ^h	0.73 ± 0.03 ^h
t	6.466	3.056	5.644	4.503	15.853
P	0.003	0.038	0.001	0.011	<0.001

Table 9. Comparison of cell migration, invasion and EMT-related protein expression in each group (n = 3, x ± s). ^bP < 0.01 versus NC-mimic; ^dP < 0.01, versus miR-200b-3p mimic + oe-NC; ^fP < 0.01, versus NC-inhibitor; ^hP < 0.01 versus NC-inhibitor.

also observed that the overexpression of miR-200b-3p significantly inhibited the expression of mesenchymal markers N-cadherin and Vimentin while promoting the expression of the epithelial marker E-cadherin, which is consistent with the aforementioned studies. Notably, this study is the first to find that the inhibitory effect of miR-200b-3p on EMT in EC cells can be reversed by the overexpression of FOSL2. FOSL2 has been shown to promote EMT, invasion, and migration in non-small cell lung cancer cells³⁰. Our study extends this finding to the field of EC.

There may be a complex interplay between miR-200b-3p and FOSL2, which plays a key role in regulating the epithelial-mesenchymal transition (EMT) process in endometrial cancer (EC) cells. Additionally, our results are consistent with the study by Xie et al.³¹ in prostate cancer, where they found that prostate leucine zipper (PrLZ) inhibits the expression of miR-200 family members through the transforming growth factor beta 1 (TGF-β1)/p-SMAD2 pathway, thereby negatively regulating ZEB1 and inducing EMT. Although this study did not directly investigate the role of the TGF-β1/p-SMAD2 pathway in EC, our findings suggest the broad and

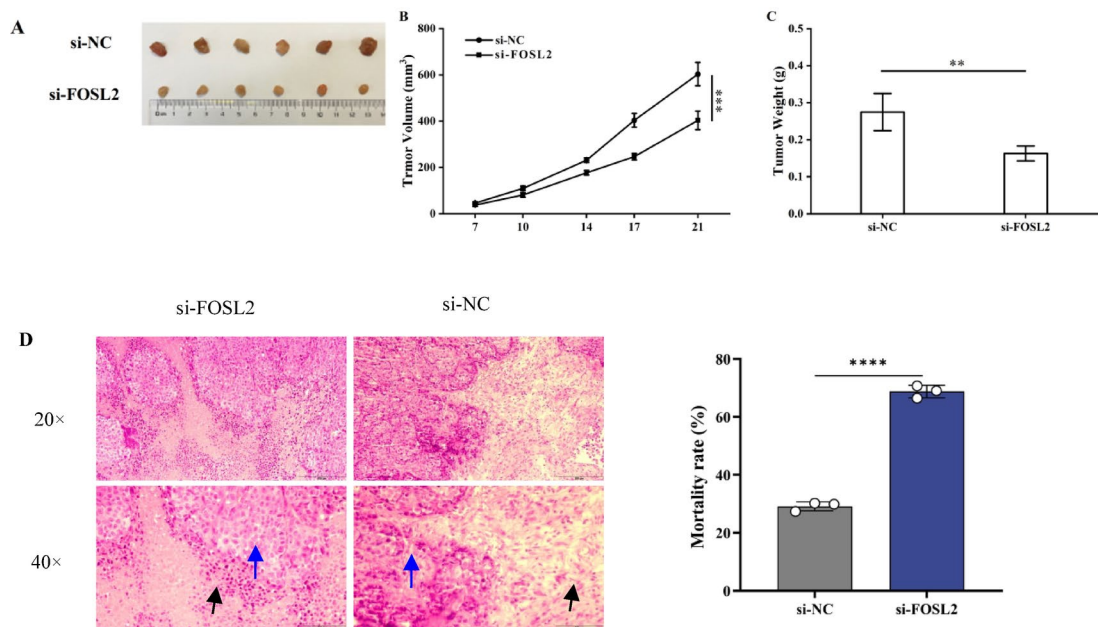


Fig. 4. Downregulation of FOSL2 significantly inhibits tumor growth. (A) tumor photos; (B) tumor growth curve; (C) tumor volume. (D) HE staining. $**P < 0.01$, $***P < 0.001$.

complex regulatory roles of miR-200 family members in EMT, potentially involving multiple signaling pathways and transcription factor interactions.

In summary, the downregulation of miR-200b-3p in EC cells may inhibit cell proliferation, invasion, and migration by regulating the EMT process, and this mechanism is associated with its targeted negative regulation of FOSL2 expression. The animal experiments in this study further confirmed that low expression of FOSL2 can inhibit the growth of endometrial cancer tumors. Targeting the miR-200b-3p/FOSL2 axis may provide new therapeutic strategies and targets for EC. Future research still needs to further explore the specific mechanisms of miR-200b-3p and FOSL2 in the occurrence and development of EC, as well as their interactions with other signaling pathways.

Data availability

All data generated or analysed during this study are included in this published article.

Received: 6 August 2024; Accepted: 25 April 2025

Published online: 06 May 2025

References

- Crosbie, E. J. et al. Endometrial cancer. *Lancet* **399**, 1412–1428. [https://doi.org/10.1016/S0140-6736\(22\)00323-3](https://doi.org/10.1016/S0140-6736(22)00323-3) (2022).
- Ge, J., Fader, A. N. & Dudley, J. C. Early detection of endometrial cancer. *Gynecol. Oncol.* **174**, A1–A2. <https://doi.org/10.1016/j.gyno.2023.06.001> (2023).
- Yen, T. T. et al. Molecular classification and emerging targeted therapy in endometrial cancer. *Int. J. Gynecol. Pathol.* **39**(1), 26–35. <https://doi.org/10.1097/PGP.0000000000000551> (2020).
- Cronin, K. A. et al. Annual report to the nation on the status of cancer, part 1: National cancer statistics. *Cancer* **128**(24), 4251–4284. <https://doi.org/10.1002/cncr.34354> (2022).
- Hill, M. & Tran, N. miRNA interplay: Mechanisms and consequences in cancer. *Dis Model Mech.* **14**(4), 047662. <https://doi.org/10.1242/dmm.047662> (2021).
- Sengupta, D. et al. Dissecting miRNA facilitated physiology and function in human breast cancer for therapeutic intervention. *Semin. Cancer Biol.* **72**, 46–64. <https://doi.org/10.1016/j.semcancer.2021.05.001> (2021).
- Safavi, P. et al. Interplay between lncRNA/miRNA and TGF- β signaling in the tumorigenesis of gynecological cancer. *Curr. Pharm. Des.* **30**(5), 352–361. <https://doi.org/10.2174/1389201029666230215111551> (2024).
- Wang, Q. et al. Novel miRNA markers for the diagnosis and prognosis of endometrial cancer. *J. Cell. Mol. Med.* **24**(8), 4533–4546. <https://doi.org/10.1111/jcmm.15227> (2020).
- Chen, C., Zhang, Q. & Kong, B. miRNA-576-5p promotes endometrial cancer cell growth and metastasis by targeting ZBTB4. *Clin. Transl. Oncol.* **25**(3), 706–720. <https://doi.org/10.1007/s12094-022-02952-3> (2023).
- Cavallari, I. et al. The miR-200 family of microRNAs: Fine tuners of epithelial-mesenchymal transition and circulating cancer biomarkers. *Cancers* **13**(23), 5874. <https://doi.org/10.3390/cancers13235874> (2021).
- Chen, S. et al. Regulatory functions of miR-200b-3p in tumor development (Review). *Oncol. Rep.* **47**(5), 96. <https://doi.org/10.3892/or.2022.8328> (2022).
- Yang, C. et al. Circ_0007331 promotes the PTX resistance and progression of breast cancer via miR-200b-3p/ANLN. *J. Surg. Res.* **279**, 619–632. <https://doi.org/10.1016/j.jss.2022.06.043> (2022).
- Xu, Y. et al. Exosomal miR-200b-3p induces macrophage polarization by regulating transcriptional repressor ZEB1 in hepatocellular carcinoma. *Hepatol. Int.* **17**(4), 889–903. <https://doi.org/10.1007/s12072-023-00544-6> (2023).

14. Bian, Z. et al. SNHG17 promotes colorectal tumorigenesis and metastasis via regulating Trim23-PES1 axis and miR-339-5p-FOSL2-SNHG17 positive feedback loop. *J. Exp. Clin. Cancer Res.* **40**(1), 360. <https://doi.org/10.1186/s13046-021-02092-1> (2021).
15. Chen, X. et al. Retraction notice to: lncRNA UCA1 promotes gefitinib resistance as a ceRNA to target FOSL2 by sponging miR-143 in non-small cell lung cancer. *Mol. Ther. Nucleic Acids* **35**(2), 102215. <https://doi.org/10.1016/j.omtn.2024.01.005> (2024).
16. Hu, Y. et al. lncRNA GSTM3TV2 promotes cell proliferation and invasion via miR-597/FOSL2 axis in hepatocellular carcinoma. *Biomed. Res. Int.* **2021**, 3445970. <https://doi.org/10.1155/2021/3445970> (2021).
17. Yu, L., Zhang, F. & Wang, Y. Circ_0005615 regulates the progression of colorectal cancer through the miR-873-5p/FOSL2 signaling pathway. *Biochem. Genet.* **61**(5), 2020–2041. <https://doi.org/10.1007/s10528-023-00415-4> (2023).
18. Chen, W. et al. Differentially expressed microRNA in prognosis of gastric cancer with Lauren classification. *Cancer Biomark.* **41**(1), 41–54. <https://doi.org/10.3233/CBM-220226> (2024).
19. Ma, X. et al. circKDM4C enhances bladder cancer invasion and metastasis through miR-200b-3p/ZEB1 axis. *Cell. Death Discov.* **7**(1), 365. <https://doi.org/10.1038/s41420-021-00506-8> (2021).
20. Kim, D. H. et al. Identification of exosomal microRNA panel as diagnostic and prognostic biomarker for small cell lung cancer. *Biomark. Res.* **11**(1), 80. <https://doi.org/10.1186/s40364-023-00550-6> (2023).
21. Wang, X. et al. miR-200b-3p accelerates progression of pituitary adenomas by negatively regulating expression of RECK. *Oncol. Res.* **32**(5), 933–941. <https://doi.org/10.3727/096504021X16373485825804> (2024).
22. Gytyte, U. et al. The role of miR-375-3p and miR-200b-3p in gastrointestinal stromal tumors. *Int. J. Mol. Sci.* **21**(14), 5151. <https://doi.org/10.3390/ijms21145151> (2020).
23. Wan, X. et al. FOSL2 promotes VEGF-independent angiogenesis by transcriptionally activating Wnt5a in breast cancer-associated fibroblasts. *Theranostics* **11**(10), 4975–4991. <https://doi.org/10.7150/thno.49096> (2021).
24. Ma, W. et al. Circ-FAT1 up-regulates FOSL2 expression by sponging miR-619-5p to facilitate colorectal cancer progression. *Biochem. Genet.* **60**(4), 1362–1379. <https://doi.org/10.1007/s10528-022-00345-6> (2022).
25. Gao, L. et al. Silencing circRNA001937 may inhibit cutaneous squamous cell carcinoma proliferation and induce apoptosis by preventing the sponging of the miRNA-597-3p/FOSL2 pathway. *Int. J. Mol. Med.* **46**(5), 1653–1660. <https://doi.org/10.3892/ijmm.2020.4663> (2020).
26. Chen, Q. et al. lncRNA TUG1 promotes the migration and invasion in type I endometrial carcinoma cells by regulating E-N cadherin switch. *Taiwan J. Obstet. Gynecol.* **61**(5), 780–787. <https://doi.org/10.1016/j.tjog.2022.05.004> (2022).
27. Paolillo, M. & Schinelli, S. Extracellular matrix alterations in metastatic processes. *Int. J. Mol. Sci.* **20**(19), 4947. <https://doi.org/10.3390/ijms20194947> (2019).
28. Mortezaee, K., Majidpoor, J. & Kharazinejad, E. Epithelial-mesenchymal transition in cancer stemness and heterogeneity: updated. *Med. Oncol.* **39**(12), 193. <https://doi.org/10.1007/s12032-022-01801-0> (2022).
29. Akrida, I. et al. Epithelial to mesenchymal transition (EMT) in metaplastic breast cancer and phyllodes breast tumors. *Med. Oncol.* **41**(1), 20. <https://doi.org/10.1007/s12032-023-01926-0> (2023).
30. Rhodes, L. V. et al. Dual regulation by microRNA-200b-3p and microRNA-200b-5p in the inhibition of epithelial-to-mesenchymal transition in triple-negative breast cancer. *Oncotarget* **6**(18), 16638–16652. <https://doi.org/10.18632/oncotarget.4102> (2015).
31. Xie, H. et al. PriZ regulates EMT and invasion in prostate cancer via the TGF- β 1p-SMAD2/miR-200 family/ZEB1 axis. *Prostate* **84**(4), 317–328. <https://doi.org/10.1002/pros.26196> (2024).

Author contributions

(I) Conception and design: Lijie He; (II) Administrative support: Zhe Han; (III) Provision of study materials or patients: Zhongmin Jiang; (IV) Data analysis and interpretation: Jing Wang; (V) Manuscript writing: All authors; (VI) Final approval of manuscript: All authors.

Funding

Research Innovation and Translation Fund of Tianjin Fifth Central Hospital (Grant No.2024-CX-06) Sponsored by Tianjin Binhai New Area Health Research Project (Grant No.2023 BWKQ003), Tianjin Health Technology Project (Grant No.TJWJ2023MS053), Tianjin Key Medical Discipline(Specialty) Construction Project (TJYX-ZDXK-062B, TJYXZDXK-079D) .

Declarations

Competing interests

The authors declare no competing interests.

Ethics approval and consent to participate

This study was approved by the Tianjin Fifth Central Hospital Ethics Committee, I confirmed that informed consent was obtained from all patients and their families, I confirmed all methods were carried out in accordance with Helsinki declaration. I confirmed that all experiments in this study were performed in accordance with the relevant guidelines and regulations. All the procedure of the study is followed by the ARRIVE (Animal Research: Reporting In Vivo Experiments) guidelines.

Consent for publication

All authors consent for publication.

Additional information

Supplementary Information The online version contains supplementary material available at <https://doi.org/10.1038/s41598-025-00224-x>.

Correspondence and requests for materials should be addressed to Z.H.

Reprints and permissions information is available at www.nature.com/reprints.

Publisher's note Springer Nature remains neutral with regard to jurisdictional claims in published maps and institutional affiliations.

Open Access This article is licensed under a Creative Commons Attribution-NonCommercial-NoDerivatives 4.0 International License, which permits any non-commercial use, sharing, distribution and reproduction in any medium or format, as long as you give appropriate credit to the original author(s) and the source, provide a link to the Creative Commons licence, and indicate if you modified the licensed material. You do not have permission under this licence to share adapted material derived from this article or parts of it. The images or other third party material in this article are included in the article's Creative Commons licence, unless indicated otherwise in a credit line to the material. If material is not included in the article's Creative Commons licence and your intended use is not permitted by statutory regulation or exceeds the permitted use, you will need to obtain permission directly from the copyright holder. To view a copy of this licence, visit <http://creativecommons.org/licenses/by-nc-nd/4.0/>.

© The Author(s) 2025